Contents lists available at ScienceDirect

Nuclear Engineering and Technology

journal homepage: www.elsevier.com/locate/net

Original Article

Sorption of U(VI) on MX-80 bentonite, illite, shale and limestone in Na–Ca–Cl saline solutions

Zhiwei Zheng [a], Jianan Liu [a], Shinya Nagasaki [a,*], Tammy Yang (Tianxiao) [b]

[a] McMaster University, 1280 Main Street West, Hamilton, ON, L8S 4L7, Canada
[b] Nuclear Waste Management Organization, 22 St. Clair Ave. East, 4th Floor, Toronto, ON, M4T 2S3, Canada

ARTICLE INFO

ABSTRACT

Uranium (U) has been identified as an element of interest for the safety assessment of a deep geological repository for used nuclear fuel. In this study, the sorption of U(VI) was studied in Na–Ca–Cl solutions at ionic strengths = 0.1–6 mol/kgw (m) in a CO_2 free environment at pH_m (molal H^+ concentration where $pH_m = -\log m_{H^+}$) = 4–9 for MX-80 bentonite, illite and Queenston shale and at pH_m = 5–9 for limestone. U(VI) sorption on MX-80 bentonite increased with pH_m from pH_m = 4 to 6, then decreased with pH_m until pH_m = 7, and then increased again with pH_m to pH_m = 9. U(VI) sorption on illite increased with pH_m reaching a maximum at pH_m = 7, and then decreased with further increases in pH_m. The sorption behavior of U(VI) on shale was similar to that of illite, but the extent of decrease in the sorption coefficient (R_d) value with pH_m was slightly more pronounced for the shale than observed for sorption on illite at $pH_m > 7$. U(VI) sorption on limestone increased with pH_m up to pH_m = 8 and then seemed to be constant at pH_m = 8–9. U(VI) sorption on all four solids was independent of ionic strength (0.1–6.0 m). The 2 site protolysis non-electrostatic surface complexation and cation exchange model successfully simulated the sorption of U(VI) onto MX-80 and illite, and the optimized values of surface complexation constants were estimated.

1. Introduction

Sorption of radionuclides on the engineered barrier materials (e.g., bentonite) in the near-field of a deep geological repository (DGR) for nuclear fuel waste and on the host rock is a potential retardation process for migration of radionuclides to the surface [1–3]. Therefore, understanding the sorption behaviors of radionuclides on bentonite clay and host rock is important for the performance assessment of the deep geological repository. The potential host rock for a DGR in sedimentary rock in Canada consists of shale and limestone [4]. Bentonite clay will be used in the engineered barrier system as a buffer/backfill material for such a DGR [4]. Therefore, this paper explores the sorption of uranium on shale, limestone, MX-80 bentonite and illite under potential repository conditions in a sedimentary rock environment in Canada.

Uranium (U) is a major radionuclide in the used nuclear fuel waste and a parent element of many radioactive daughter elements. Used nuclear fuel wastes will be safely contained in copper-coated steel containers and isolated in the deep geological repository for the long-term. Over the lifetime of the repository after repository closure, groundwater will be expected to eventually reach the engineered

barriers. In the event that a waste container fails, groundwater can contact the waste form and uranium (in the UO_2 matrix) will be dissolved into the groundwater. The possible maximum concentration of uranium in the near field of the repository will be determined by the solubility of UO_2 under reducing conditions expected at the repository depth. Under oxidizing conditions, U may assume the oxidized U(VI) state which can be more mobile in aqueous solution than its reduced U (IV) state. Hence, we focused on the study of the sorption of U(VI) species in this work.

In this paper, we studied the sorption of U(VI) on MX-80 bentonite, illite which is considered the major sorbing mineral of shale, Queenston shale and limestone in Na–Ca–Cl solutions with ionic strengths (I) of 0.1–6 mol/kgw (m) as well as in the reference groundwater SR-270-PW, which represents the potential groundwater geochemical conditions at the repository depth of Canadian sedimentary rock [5]. SR-270-PW is a Na–Ca–Cl type water containing HCO_3^- with a total dissolved solid concentration of 275 g/L or $I = 6$ m [6]. The Na/Ca mole ratio of the Na–Ca–Cl solutions was 2.7 which is the same as that of the SR-270-PW reference groundwater.

There are many previous studies on the sorption of U(VI) onto

---

* Corresponding author.
E-mail address: nagasas@mcmaster.ca (S. Nagasaki).

bentonite/montmorillonite [7–19] and illite [20–26] and some studies on the sorption of U(VI) onto shale and limestone [27–30]. The most relevant previous studies are summarized here [8,11,19,20,26]. The proposed surface complexation reactions and surface complexation constants (log K^0) on strong and weak sites and the range of sorption of U(VI) reported in those studies are summarized in Table 1. Bradbury and Baeyens [8] applied a 2 site protolysis non-electrostatic surface complexation and cation exchange (2SPNE SC/CE) model to the pH dependence of sorption data for Mn(II), Co(II), Ni(II), Zn(II), Cd(II), Eu (III), Am(III), Sn(IV), Th(IV), Np(V) and U(VI) which were measured by the authors or taken from the literature. Surface complexation constants on montmorillonite were evaluated and equations of linear free energy relationships (LFER) were derived. The sorption of U(VI) on Na-SWy-1 bentonite in 0.01 and 0.1 mol/L (M) NaClO$_4$ solutions and on Na-SAz-1 bentonite in 0.1 M NaClO$_4$ solution was studied [8]. Marques Fernandes et al. [11] studied the sorption mechanisms of U(VI) on montmorillonite (Na-SWy-1) in 0.1 M NaClO$_4$ solution in the absence and presence of carbonate by sorption experimental measurements, using 2SPNE SC/CE sorption modeling and the extended X-ray absorption fine structure spectroscopy (EXAFS) technique. From the pH dependence of sorption and the sorption isotherms at pH = 5, 6.8 and 8 in the absence of carbonate, the surface complexation reactions were discussed and the surface complexation constants on strong sites were evaluated. Marques Fernandes et al. [11] also evaluated the surface complexation constants on weak sites. In the presence of carbonate, Marques Fernandes et al. [11] found that two surface complexation reactions on strong sites and one on weak sites were necessary to reproduce the experimental data. Stockmann et al. [19] studied the effect of I (0.1–3 m NaCl or CaCl$_2$ solutions) on the sorption of U(VI) onto SWy-2 as a function of pH$_c$ (molar H$^+$ concentrations (pH$_c$ = −log c_{H+})) in the absence and presence of CO$_2$ in the experimental atmosphere. A combination of batch sorption experiments with time-resolved laser-induced fluorescence spectroscopy and *in situ* attenuated total reflection Fourier-transform infrared (ATR FT-IR) spectroscopy was applied to elucidate the sorption mechanisms. The 2SPNE SC/CE model was applied to their experimental data and the literature sorption data. In addition, Pabalan and Turner [7] studied the sorption of U(VI) on montmorillonite in 0.1 M NaNO$_3$ solution in equilibrium with atmospheric P_{CO2} to elucidate the effect of pH (2–9) on sorption. Majdan et al. [9] studied the sorption of U(VI) on bentonite which was modified by hexadecyltrimethylammonium bromide in uranyl acetate solutions with the initial U(VI) concentration ranging from 0.0001 to 0.001 M at pH = 3–10. Ren et al. [10] examined the dependence of the sorption of U(VI) onto MX-80 bentonite on contact time (1–24 h), pH (2–8), I (0.001–0.1 M NaClO$_4$ solutions), solid contents (0.2–1.3 g/L), humic and fulvic acids (0–20 mg/L) and temperature (303–333 K). Xiao et al. [12] studied the dependence of sorption of U(VI) on bentonite sampled from Huangshan County (China) on pH (2–10) and I (0.001–0.1 M NaClO$_4$, 0.01 M LiClO$_4$, 0.01 M KClO$_4$ solutions). Verma et al. [13] studied the sorption of U(VI) onto bentonite clay at pH = 2–8 and I = 0.01–1 M NaClO$_4$ solutions. Li et al. [14] studied the dependence of sorption and desorption of U(VI) onto GMZ bentonite on pH (2–11) and I = 0–0.1 M (in the absence of NaCl, 0.01–0.1 M NaCl, 0.001–0.1 M KCl, and 0.01 M LiCl solutions). Zheng et al. [15] studied the sorption of U(VI) on GMZ bentonite in the absence and presence of fulvic acid at pH = 2–8 in 0.02–0.1 M NaCl solutions. Zuo et al. [16] investigated the effect of thermal activation on the sorption of U(VI) onto bentonite in NaCl solutions with I = 0.001–0.5 M. Philipp et al. [17] studied the sorption of U (VI) on Ca-bentonite in a mixed salt solution with I = 2.63 M (2.5 M NaCl + 0.02 M CaCl$_2$ + 0.02 M Na$_2$SO$_4$ + 0.0051 M KCl solutions) in the pH range 8–13 at different carbonate concentrations. Brix et al. [18] studied the effect of the initial U(VI) concentration (5×10^{-9} – 2.5×10^{-4} M) on U(VI) sorption on Ca-bentonite at pH = 12.5 (artificial cement pore water) and pH = 13 (0.1 M, 1 M and 5 M NaCl solutions).

For the sorption of U(VI) on illite, Bradbury and Baeyens [20] studied the sorption of U(VI) on purified Na-illite du Puy in 0.1 M

Table 1

Surface complexation reactions, surface complexation constants (log K^0) and range of sorption of U(VI) on bentonite/montmorillonite and illite reported in the previous studies.

Bentonite/Montmorillonite

Surface complexation reaction		log K^0 [8]	log K^0 [11]	log K^0 [19]
Strong site	$\equiv$SOH + UO$_2^{2+}$ $\rightleftarrows$ $\equiv$SOUO$_2^+$ + H$^+$	3.1	3.1	2.42
	$\equiv$SOH + UO$_2^{2+}$ + H$_2$O $\rightleftarrows$ $\equiv$SOUO$_2$OH + 2H$^+$	- 3.4	- 4.6	- 4.49
	$\equiv$SOH + UO$_2^{2+}$ + 2H$_2$O $\rightleftarrows$ $\equiv$SOUO$_2$(OH)$_2$ + 3H$^+$	- 11.0	- 12.6	–
	$\equiv$SOH + UO$_2^{2+}$ + 3H$_2$O $\rightleftarrows$ $\equiv$SOUO$_2$(OH)$_3^-$ + 4H$^+$	- 20.5	- 20.9	- 20.5
	$\equiv$SOH + UO$_2^{2+}$ + CO$_3^{2-}$ $\rightleftarrows$ $\equiv$SOUO$_2$CO$_3^-$ + H$^+$	–	9.8	–
	$\equiv$SOH + UO$_2^{2+}$ + 2CO$_3^{2-}$ $\rightleftarrows$ $\equiv$SOUO$_2$(CO$_3$)$_2^{3-}$ + H$^+$	–	15.5	–
Weak site	$\equiv$SOH + UO$_2^{2+}$ $\rightleftarrows$ $\equiv$SOUO$_2^+$ + H$^+$	0.7	0.5	–
	$\equiv$SOH + UO$_2^{2+}$ H$_2$O $\rightleftarrows$ $\equiv$SOUO$_2$OH + 2H$^+$	- 5.7	- 5.7	–
	$\equiv$SOH + UO$_2^{2+}$ + CO$_3^{2-}$ $\rightleftarrows$ $\equiv$SOUO$_2$CO$_3^-$ + H$^+$	–	9.3	–
Range of R_d (mL/g) or U(VI) immobilized (%) in the absence of CO$_2$		1.6×10^3 ~ 4.0×10^5 (mL/g) in 0.01 M NaClO$_4$ 1.0×10^2 ~ 2.5×10^5 (mL/g) in 0.1 M NaClO$_4$	1.0×10^2 ~ 2.5×10^5 (mL/g) in 0.1 M NaClO$_4$	95 ~ 100 (%) in 0.3 m NaCl 89 ~ 99 (%) in 1 m NaCl 84 ~ 99 (%) in 3 m NaCl 89 ~ 99 (%) in 0.3 m CaCl$_2$ 86 ~ 99 (%) in 1 m CaCl$_2$ 75 ~ 99 (%) in 3 m CaCl$_2$
Experimental conditions of CO$_2$		In the absence of CO$_2$	In the absence of CO$_2$, atmospheric pCO$_2$, or 1, 3 and 5 mM NaHCO$_3$	In the absence of CO$_2$, or atmospheric pCO2
Solution/Ionic strength		0.01 M NaClO$_4$ 0.1 M NaClO$_4$	0.1 M NaClO$_4$	0.1–3 m NaCl 0.1–3 m CaCl$_2$

Illite

Surface complexation reaction		log K^0 [20]	log K^0 [26]
Strong site	SOH + UO$_2^{2+}$ $\rightleftarrows$ SOUO$_2^+$ + H$^+$	2	–
	SOH + UO$_2^{2+}$ + H$_2$O $\rightleftarrows$ SOUO$_2$OH + 2H$^+$	- 3.5	–
	SOH + UO$_2^{2+}$ + H$_2$O $\rightleftarrows$ SOUO$_2$(OH)$^-$ + 3H$^+$	- 10.6	–
	SOH + UO$_2^{2+}$ + 3H2O $\rightleftarrows$ SOUO$_2$(OH)$_3^-$ + 4H$^+$	- 19.0	–
	$\equiv$SOH + UO$_2^{2+}$ + CO$_3^{2-}$ $\rightleftarrows$ $\equiv$SOUO$_2$CO$_3^-$ + H$^+$	–	11.7 ± 0.2
	$\equiv$SOH + UO$_2^{2+}$ + 2CO$_3^{2-}$ $\rightleftarrows$ $\equiv$SOUO$_2$(CO$_3$)$_2^{3-}$ + H$^+$	–	17.0 ± 0.1
Range of R_d (mL/g)		1.2 ~ 7.9×10^4 (mL/g) in 0.1 M NaClO$_4$	1.1×10^{-2} ~ 1.4×10^{-1} (mL/g) in air 7.1×10^{-5} ~ 7.3×10^{-3} (mL/g) in

Table 1 (*continued*)

Illite		
Surface complexation reation	log K^0 [20]	log K^0 [26]
		1 mM DIC $3.2 \times 10^{-5} \sim 8.8 \times 10^{-4}$ (mL/g) in 2 mM DIC $1.5 \times 10^{-6} \sim 1.5 \times 10^{-4}$ (mL/g) in 5 mM DIC $1.5 \times 10^{-6} \sim 8.4 \times 10^{-5}$ (mL/g) in 10 mL DIC
Experimental conditions of CO_2	In the absence of CO_2	1.0, 2.0, 5.0, 10, 100, and 250 mM
Solution/Ionic strength	0.1 M NaClO$_4$	0.1 M NaCl

Note: R_d is sorption distribution coefficient (mL/g).

NaClO$_4$ solution at pH = 2–10 and applied a 2SPNE SC/CE model to the sorption data. By considering one cation exchange reaction and four surface complexation reactions, Bradbury and Baeyens [20] successfully reproduced the sorption experimental results. Bradbury and Baeyens [20] also proposed a LFER. Mei et al. [26] studied the effect of dissolved inorganic carbon (DIC; up to 250 mM) and pH (7–11) on the sorption of U(VI) onto illite du Puy in 0.1 M NaCl solution using batch sorption experiments, surface complexation modeling, and time-resolved laser fluorescence spectroscopy (TRLFS). The sorption coefficient (R_d) values were found to decrease with increasing DIC concentration. The 2SPNE SC/CE model showed that two surface complexation reactions between strong sites and carbonate were needed to reproduce the experimental data. In addition, Marques Fernandes et al. [21] measured the sorption isotherms of U(VI) for Boda and Opalinus Clay in 0.1 M NaClO$_4$ solution at pH 8.1 and 7.7, respectively, and used the U(VI) isotherm on Na-illite at pH = 5.8 in 0.1 M NaClO$_4$ solution from reference [22]. Gao et al. [23] studied the sorption of U(VI) on illite in I = 0.001 M, 0.01 M and 0.1 M NaNO$_3$ solutions at pH = 3.5–9.5. Liao et al. [24] studied the dependence of sorption of U(VI) onto illite on pH (3–10), sorbent dosage (0.20–50 g/L), total phosphorus concentration (0–2 mg/L), initial uranium concentration (0.10–70 mg/L), shaking time (0.08–48 h), temperature (298–323 K) and uranium species in the NaCl solution (0.02–1 M with phosphorus concentration = 0–2 mg/L). Montavon et al. [25] studied the effects of pH (4–10), P_{CO2} ($10^{-3.5}$, 10^{-2}, $10^{-1.3}$ atm), and redox potential (U(VI) and U(IV)) on sorption of uranium onto illite and Callovo-Oxfordian Clay (COx) formation in synthetic pore water of COx formation (with I = 0.08 M) and in 0.1 M NaNO$_3$ and 0.1 M NaCl solutions.

For the sorption of U(VI) on shale and limestone, Zhang et al. [27] studied the uptake of U(VI) on weathered shale/limestone saprolite in 0.05 M NaNO$_3$ solution at equilibrium with atmospheric CO_2 at solid/liquid ratio = 0.005 and 0.25 kg/L. They applied Ferrihydrite model, Stepwise Regression method and Simultaneous Regression method to the batch sorption experimental results and studied how the surface complexation constants, uncertainties and errors were affected by the different models they applied. Ortaboy and Atun [28] studied the dependence of sorption of U(VI) onto a bituminous shale from the Black Sea region in NaOH and Na$_2$CO$_3$ solutions on contact time (up to around 250 min), adsorbent dosage (2–40 g/L), initial U(VI) concentration (0.1–1 mM), pH (3.69–11.64 in NaOH solution, and 3.89–8.15 in Na$_2$CO$_3$ solution) and temperature (298, 318 and 338 K). The effect of pH on U(VI) sorption was measured in 0.1, 1.0, 5.0 and 10 mM NaOH or Na$_2$CO$_3$ solutions. Kim et al. [29] studied the sorption of U(VI) on saprolite derived from interbedded shale, limestone, and sandstone sequences in 0.05 M NaNO$_3$ solution in the presence of CO$_3^{2-}$. Zuo et al. [30] studied the effects of pH (4–10), initial uranium concentration (100–300 μg/mL), rock particle size (0.12–0.25 mm) and solid/liquid ratio (0.25–1 g/30 mL) on the sorption of U(VI) on shale in Ca–HCO$_3$

type water with salinity = 319 mg/L.

However, to the best of our knowledge, there is no previous research that investigated the effects of pH and I on U(VI) sorption onto bentonite, illite, shale or limestone over the wide range of pH and I, except the work by Stockmann et al. [19]. Stockmann et al. [19] studied U(VI) sorption onto SWy-2 montmorillonite in the I of 0.1–3 m NaCl and CaCl$_2$ solutions at pH$_c$ of 4–10 in NaCl solution and 4–9 in CaCl$_2$ solution.

In this study, sorption of U(VI) was systematically investigated in Na–Ca–Cl solutions with I = 0.1–6 m at pH$_m$ (molal H$^+$ concentration where pH$_m$ = $-\log m_{H+}$)) = 4–9 for MX-80 bentonite, illite and shale and at pH$_m$ = 5–9 for limestone using batch experiments. The sorption of U (VI) on limestone was not investigated at pH$_m$ = 4–5 because it was difficult to adjust the pH$_m$ value of solutions containing limestone to around 4. For the sorption of U(VI) on MX-80 bentonite and illite, the 2SPNE SC/CE model was applied to examine the surface complexation reactions and estimate the optimized values of surface complexation constants, log K^0.

2. Experimental

2.1. Materials

All chemicals used in this work were ACS reagent grade. HCl (CAS 7647-01-0, assay: 36.5–38.0 %), NaOH (CAS 1310-73-2, assay: ≥97.0 %), KCl (CAS 7447-40-7, assay: 99.0–100.5 %), NaCl (CAS 7647-14-5, assay: ≥99.0 %), CaCl$_2$•2H$_2$O (CAS 10035-04-8, assay: 99.0–105.0 %), MgCl$_2$•6H$_2$O (CAS 7791-18-6, assay: 99–101 %) and KBr (CAS 7758-02-3, assay: ≥99.0 %) were purchased from Fisher Scientific and SrCl$_2$•6H$_2$O (CAS 10025-70-4, assay: 99.0 %/99.0–103.0 % (ACS specification)), NaHCO$_3$ (CAS 144-58-8, assay: ≥99.7 %) and Na$_2$SO$_4$ (CAS 7757-82-6, assay: ≥99.0 %) were from Millipore Sigma. Deionized water used was prepared with a Milli-Q Direct 8 (18.2 MΩ/cm) system.

The four solids used in the sorption experiments were Volclay MX-80 Na-bentonite (provided by American Colloid Company (ACC), from Wyoming, USA; about 80 wt% Na-rich montmorillonite), IMt-2 Na-illite (provided by Clay Mineral Society, from Silver Hill, USA), and Queenston shale (DGR5-548.02) and limestone (DGR5-729.91), both sampled from the Bruce Nuclear site in Ontario, Canada and provided by the Nuclear Waste Management Organization (NWMO). The illite, shale, and limestone samples were crushed and sieved to a particle size of 150–300 μm. According to the ACC, the MX-80 bentonite has particle sizes ranging from 74 to 420 μm and was used as received. The surface properties of MX-80 bentonite and illite such as protolysis reaction constants, surface site capacities and specific surface areas are summarized in our previous paper on the Se(-II) sorption on MX-80 bentonite and illite [31]. Preliminary experiments were conducted to determine if any uranium will dissolve from the four solids (bentonite, illite, shale and limestone) during the batch sorption testing. Each solid sample (1 g) was mixed with deionized water (10 mL), stirred once a day for about 10 min, and left to stand for two weeks. After two weeks, the solid sample was separated from the liquid phase by centrifugation, and the concentration of U in the liquid phase was measured by Inductively Coupled Plasma Mass Spectrometry (ICP-MS) (Agilent ICP-MS 8800. The detection limit of U was less than 5×10^{-12} m). We confirmed that the concentrations of U in all four liquid phases (of the four solids) were less than the detection limit of the ICP-MS. Therefore, the dissolution of U from the four solids during the sorption measurement period is negligible.

A stock solution of natural U(VI) in 0.01 M HCl solution was supplied by the Department of Health Physics, McMaster University. Na–Ca–Cl solutions (Na/Ca mole ratio = 2.7) with I = 0.1, 1, 2, 3 and 6 m were prepared using pure NaCl and CaCl$_2$•2H$_2$O compounds. The SR-270-PW reference groundwater (Na/Ca mole ratio = 2.7; I = 6 m) was prepared using the masses of reagents shown in Table 2. All reagents were dissolved into a total of 1 kg of deionized water.

Table 2
Masses of chemical compounds added to 1 kg deionized water for preparation of the SR-270-PW reference groundwater.

Compound	Mass of Compound (g)
KCl	22.2
NaCl	126.7
$CaCl_2 \bullet 2H_2O$	117.4
$MgCl_2 \bullet 6H_2O$	68.6
$SrCl_2 \bullet 6H_2O$	3.7
$NaHCO_3$	0.15
Na_2SO_4	0.65
KBr	2.5

A glove box (GB) which was filled with constant flushing N_2 gas (>99.998 %) was used to exclude CO_2. All the sorption experiments were conducted in the glove box. In this study, the sorption kinetics and the sorption experiments of the dependence of R_d on pH_m and I conducted in Na–Ca–Cl solutions were measured in the absence of CO_2. For the sorption measurements conducted in the SR-270-PW reference groundwater which contains a small amount of HCO_3^-, the test tubes were tightly sealed in the GB to control the concentration of HCO_3^-. Therefore, the R_d values of U(VI) on the four solids in SR-270-PW were measured in the presence of a small amount of HCO_3^-.

To measure pH values, we used a Fisherbrand accumet AB200 Benchtop pH meter in conjunction with a Fisherbrand accumet pH combination electrode. We completed the calibration of the pH meter using buffer solutions with pH = 4.0, 7.0, and 10.0. The pH values indicated on the pH meter ($pH_{measure}$) are operational values, therefore need to be converted to pH_m. The conversion of $pH_{measure}$ to pH_m is described elsewhere [32,33]. In this study, we assumed the relationship of $pH_{measure}$ and pH_m [32,33]: $- \log m(H^+) = pH_{measure} + A$ (where A is a function of molal concentration of Na–Ca–Cl and SR-270-PW solutions). We measured the $m(H^+)$ and $pH_{measure}$ by acid-base titration (Metrohm Ti-Touch 916) to establish the relationship between $pH_{measure}$ and pH_m for the Na–Ca–Cl and SR-270-PW solutions.

We also measured the redox potentials (Eh) of the solutions during sorption kinetics tests using a Pt combined electrode with an Ag/AgCl reference electrode (Fisher Scientific Accumet AB 150/Accumet ORP electrode) and converted those measured values into Eh versus Standard Hydrogen Electrode (SHE). It was found that the Eh values were around 300–350 mV versus SHE. Therefore, we considered that oxidizing conditions were maintained (i.e., reducing conditions were not created) under the pure N_2 atmosphere.

2.2. Sorption experiments

2.2.1. Sorption kinetics

All sorption kinetics experiments were carried out at 25 °C in the GB. The experimental procedures were the same as those established for our experiments of Np(IV) sorption in Na–Ca–Cl solutions [34]. In the present work, the R_d [mL/g] (sorption distribution coefficient) value was used to describe the results of the sorption experiment:

$$R_d = \frac{(C_0 - C_e)}{C_e} \frac{V}{W},$$

where C_0 (m) is the initial concentration of U(VI) in solution (1×10^{-6} m), C_e [m] is the U(VI) concentration in solution at sorption equilibrium, V [mL] is the volume of the solution, and W [g] is the mass of MX-80 bentonite, illite, shale or limestone being used.

The solid/liquid ratio for all sorption experiments was 0.3 g/30 mL (=10 g/L). All sorption experiments were preceded by pre-equilibration, where 30 mL of Na–Ca–Cl solution with respective I (0.1, 1, 2, 3 or 6 m) was mixed with 0.3 g MX-80 bentonite, illite, shale or limestone. After the suspension was kept in the GB for a week, the solution was separated by centrifugation (6 min at 3000 rpm) and then removed with a pipette. Then, 30 mL of the same Na–Ca–Cl solution (with the same I) was added

to the tube and spiked with the U(VI) stock solution to reach an initial U (VI) concentration of 1×10^{-6} m. The solubility of $UO_2(OH)_2$ in the 0.1 m Na–Ca–Cl solution at pH = 7 was estimated as 5×10^{-6} m using PHREEQC [35] calculations (with the JAEA (Japan Atomic Energy Agency) thermodynamic database [36]). In this study, an initial concentration of U(VI) of 1×10^{-6} m, which is lower than the solubility limit of U(VI) simulated using PHREEQC, was selected. This is also the same initial concentration used by Stockmann et al. [19] in their U(VI) sorption experiments.

The kinetic experiments for uptake of U(VI) on MX-80 bentonite, illite, shale and limestone in Na–Ca–Cl solutions were conducted for $I =$ 0.1 and 6 m. After the U(VI) stock solution was spiked, the value of pH_m was adjusted to 6.5 ± 0.3. Then, the sample tubes containing U(VI), solid and solution were tightly sealed and gently shaken at 25 °C in the GB. The value of pH_m was measured daily in the GB. When the value of pH_m changed by more than ± 0.3 from the initial value, the pH_m was re-adjusted by adding a small volume of HCl or NaOH solution. After the pre-determined period of time (e.g., 1 day, 2 days, 3 days, 7 days, 14 days and 21 days), the solution was separated from the solid by ultra-centrifugation at 100,000 rpm for 15 min, at 25 °C (Optima™ Max-XP Biosafe Ultracentrifuge System). The pH_m of the solution was measured in the GB, and an aliquot of solution was sampled and transferred to a test tube. The U(VI) concentration in the test tube was measured by ICP-MS. We measured the concentration of U(VI) in the sampled liquid phase three times per test tube and calculated three R_d values.

2.2.2. Dependence of R_d on pH_m and ionic strength

The experiments of the dependence of the R_d of U(VI) sorption in Na–Ca–Cl solutions on pH_m were measured at $pH_m = 4$–9 for MX-80 bentonite, illite and shale and at $pH_m = 5$–9 for limestone in triplicate. The sorption dependence of R_d on pH_m was measured at I of 0.1, 1, 2, 3 and 6 m. The value of pH_m of the solution was measured once a day in the GB. When the value of pH_m shifted more than ± 0.3 from the initial one, the pH_m was re-adjusted by the addition of a small amount of HCl or NaOH solution. Due to the small volume of the added HCl or NaOH solution, the effect of HCl or NaOH addition on the final concentration of U(VI) and the R_d calculation was considered to be negligibly small. As explained in the Results and Discussion section, a steady state of U(VI) sorption on all four solids was reached within 7 days, therefore the sorption equilibration time was set as 14 days for the sorption measurements of the dependence of R_d on pH_m and I.

Furthermore, R_d values of U(VI) sorption onto MX-80 bentonite, illite, shale and limestone were also measured in the SR-270-PW reference groundwater. The nominal pH_m value of SR-270-PW is 6.0 [6]. In this study, the pH_m was adjusted to 6.5 ± 0.5 (initial pH_m value). When the value of pH_m changed by more than ± 0.3 from the initial pH_m value, the pH_m was re-adjusted using a small amount of HCl or NaOH solution. Other procedures were the same as those for the sorption kinetics measurements.

3. Results and Discussion

3.1. Sorption kinetics

Fig. 1 illustrates the sorption kinetics of U(VI) on MX-80 bentonite, illite, shale and limestone measured in Na–Ca–Cl solutions at $I = 0.1$ m and 6 m. The error bars shown in Fig. 1 represent the maximum difference between the mean R_d and the individual R_d values calculated based on three replicate measurements of the U(VI) concentration remaining in the liquid phase after the experiment. In Supplementary Materials, figures showing the percentage sorbed are provided (Fig. S1) and the measured concentrations of U(VI) in the liquid phase are also summarized (Tables S1–S4). It was found that the sorption of U(VI) reached equilibrium within 7 days on all four solids at both I of 0.1 m and 6 m. Based on these results, the sorption reaction period was set as
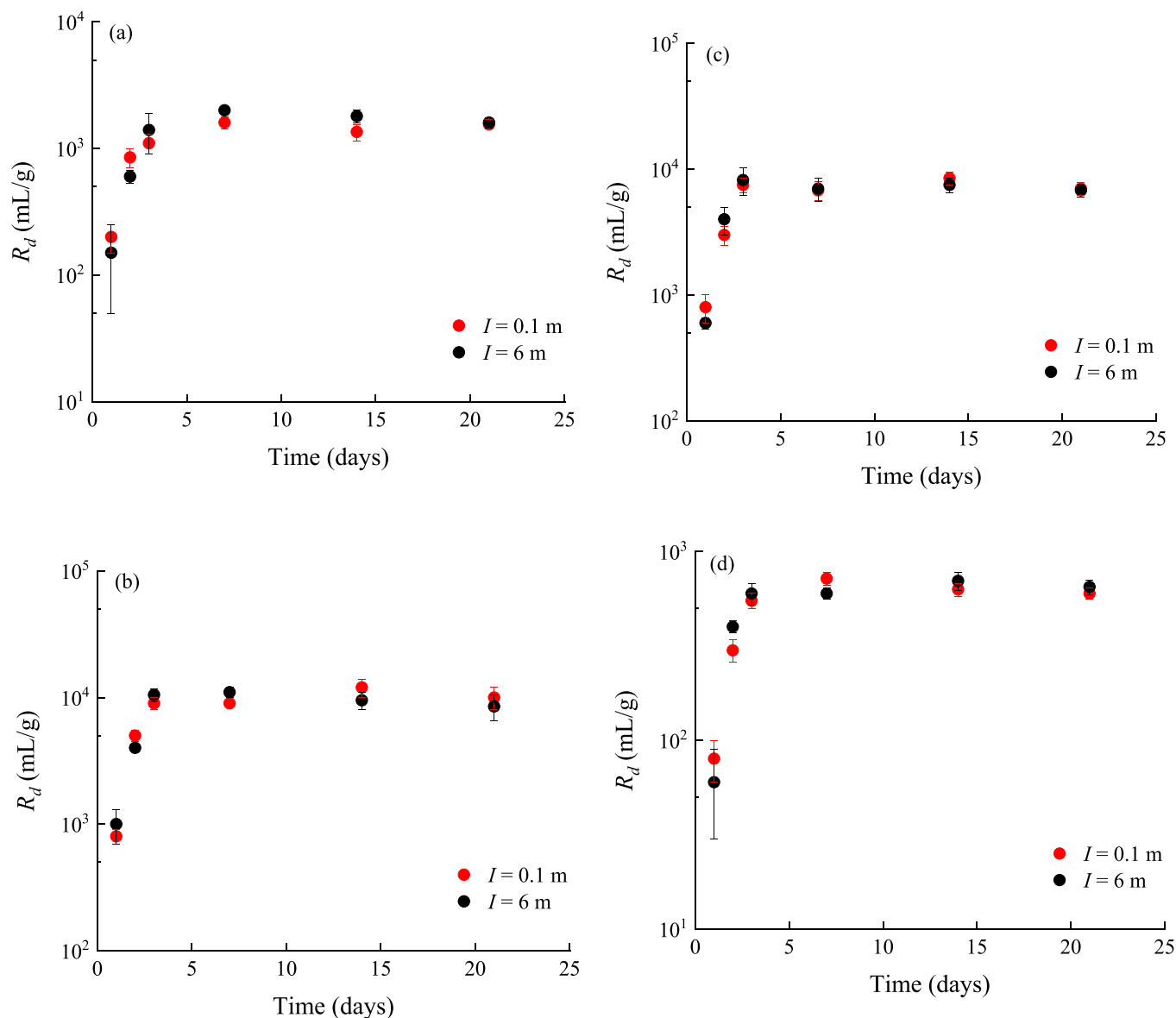
Fig. 1. Sorption kinetics of U(VI) in Na–Ca–Cl solutions at ionic strengths of 0.1 m and 6 m on (a) MX-80 bentonite, (b) illite, (c) shale, and (d) limestone. Initial concentration of U(VI) = 1 x 10^{-6} m. Solid/liquid ratio = 0.3 g/30 mL. Temperature = 25 °C. pH_m was adjusted to 6.5 ± 0.3.

14 days for experiments of the dependence of U(VI) sorption on pH_m and I for MX-80 bentonite, illite, shale and limestone.

3.2. Sorption on MX-80 bentonite

Fig. 2 plots the R_d values of U(VI) sorption on MX-80 bentonite in Na–Ca–Cl solutions at different I against pH_m (see Fig. S2 in Supplementary Materials for plots of the percentage sorbed). The R_d increased with increasing pH_m until pH_m = 6. Then, the R_d slightly decreased as pH_m increased until pH_m = 7, but R_d then increased again with pH_m to pH_m = 9. Stockmann et al. [19] observed complete U(VI) uptake on SWy-2 in the CO_2-free NaCl solution at $pH_c \geq 6$. They also observed that U(VI) uptake on SWy-2 in the CO_2-free $CaCl_2$ solution increased at $pH_c \geq 4$ with maximum values at $pH_c \geq 6$, where sorption in CO_2-free $CaCl_2$ solution was slightly lower than in the respective NaCl solution. They concluded that this slight reduction of sorption in the $CaCl_2$ solution was due to a competition of Ca^{2+} and UO_2^{2+} for sorption sites. Although the solutions Stockmann et al. [19] used were different from those used in this study, the dependence of R_d values on pH_m observed in the present study is not significantly different from the observations by Stockmann

et al. [19], except at pH_m = 6–7. The reason for a slight decrease in R_d at pH_m = 6–7 is not clear at present and would require further study.

In this study, no dependence of the R_d value on I was observed within the range of 0.1 and 6 m Na–Ca–Cl solutions. Stockmann et al. [19] observed a slight increase in U(VI) sorption with I both in the absence and presence of CO_2 from the ATR FT-IR Spectroscopy *in-situ* sorption experiment. However, similar to the results from this study, the batch sorption experiment results from Stockmann et al. [19] also showed that U(VI) sorption did not depend on I.

The R_d value of U(VI) on MX-80 bentonite in the SR-270-PW reference groundwater was estimated as 2.2 x 10^3±3.0 x 10^2 mL/g (pH_m = 6.3) and is included in Fig. 2. This is within the range of the R_d values measured in the Na–Ca–Cl solutions at pH_m = 6–7, suggesting that the impact of minor ions such as Mg^{2+}, K^+, Sr^{2+}, SO_4^{2-} and HCO_3^- on the sorption of U(VI) would be small at pH_m = 6–7.

Sorption models can be used to help to understand sorption mechanisms. Among the thermodynamic sorption models, the 2SPNE SC/CE model is the most used quasi-mechanistic model [37]. The non-electrostatic surface complexation model excludes explicit electrostatic terms in the mass action equations for surface equilibria at the
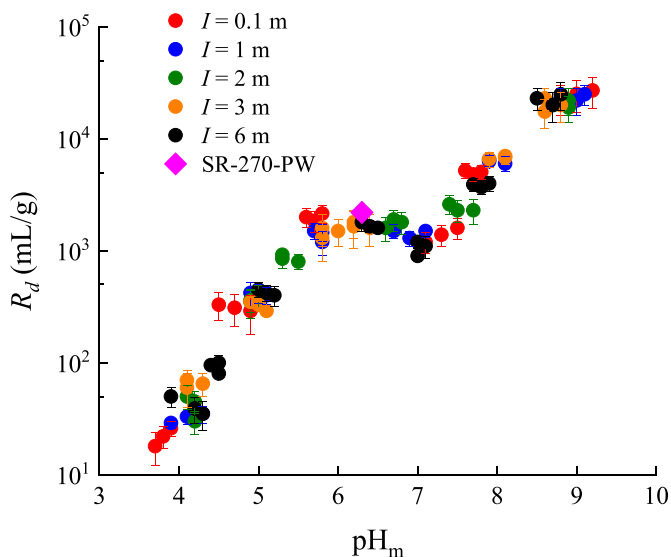
Fig. 2. pH_m and ionic strength dependences of R_d value of U(VI) sorption on MX-80 bentonite in Na–Ca–Cl solutions. Initial concentration of U(VI) = 1 x 10^{-6} m. Solid/liquid ratio = 0.3 g/30 mL. Temperature = 25 °C.

edge sites. The 2SPNE SC/CE model was firstly developed to describe the sorption behavior of divalent metals (Ni and Zn) on Na-montmorillonite [38] and has been used in a large number of studies to simulate sorption of metals onto montmorillonite and illite [e.g. 8,11,19,20]. The model is essentially a very simple one in which the pH and concentration-dependent uptake of metals onto montmorillonite and illite is described using only two amphoteric edge site types ($\equiv$SOH sites), strong and weak sites, with a fixed sorption site capacity and protonation-deprotonation constants. At trace metal concentrations, sorption is considered to occur predominantly on the strong sites. The 2SPNE SC/CE model used to simulate the uptake of aqueous metal species on montmorillonite and illite is given by the associated parameters; the selectivity coefficient of cation exchange reaction ($\log K_A^B$) and the surface complexation constants (K^0).

In this study, the 2SPNE SC/CE model incorporated in PHREEQC [35] was applied to the experimental data of the pH_m and I dependences of R_d of U(VI) sorption on MX-80 bentonite as shown in Fig. 2. The SIT (specific ion interaction theory) model was used to estimate the activity coefficients of aqueous species in solutions for $I \leq 3$ m [39]. The thermodynamic data for U(VI) was taken from the JAEA thermodynamic database [36]. In this study, the 2SPNE SC/CE model was not applied to the experimental data of $I = 6$ m which requires Pitzer thermodynamic parameters, because, to our knowledge, the Pitzer parameters included in several available Pitzer thermodynamic databases have not been fully validated yet for U(VI) in the Na–Ca–Cl system. The thermodynamic data and SIT interaction parameters used are summarized in Table S5 in Supplementary Materials. To initiate the fitting of the model to the experimental data, the values of $\log K^0$ reported by Stockmann et al. [19] were used as the initial values of constants. Values of other parameters such as protolysis constants and specific surface area were the same as those used by Walker et al. [31] and fixed during the fitting. The study by Stockmann et al. [19] considered only strong sites of montmorillonite ($\equiv S^S OH$) for modelling surface complexation at trace concentrations of U(VI) with the latest version of the 2SPNE SC/CE model which successfully predicted the experimental data [19]. The initial concentration of U(VI) used by Stockmann et al. [19] was the same as that used in this study (1 x 10^{-6} m). The solid-liquid ratio by Stockman et al. [19] was 4 g/kg-water and that in our study was 10 g/L. Since our study had a larger proportion of solid phase, we also only considered strong sites following the approach of Stockmann et al. [19]. Furthermore, the contribution of cation exchange reactions was observed to be

small at $pH_c \geq 4$ in the modelling by Stockmann et al. [19]. Therefore, we did not consider cation exchange reactions in the modelling.

The fitting results at $I = 3$ m are illustrated in Fig. 3. Other fitting results at $I = 0.1$, 1 and 2 m are shown in Supplementary Materials (Figs. S3–S5). The optimized values of $\log K^0$ for U(VI) sorption on MX-80 bentonite obtained in this study and those for U(VI) sorption on montmorillonite/bentonite obtained in other studies [8,11,19] are summarized in Table 3.

It was found that the modelling results predicted by the 2SPNE SC/CE model were consistent with the experimental results of the pH_m and I dependences of U(VI) sorption on MX-80 bentonite obtained in this study. The value of $\log K^0$ (2.3 ± 0.1) for the surface complexation reaction $\equiv SOH + UO_2^{2+} \rightleftarrows \equiv SOUO_2^+ + H^+$ optimized in this study agreed well with that reported by Stockmann et al. [19] but was smaller than those by Marques Fernandes et al. [11] and Bradbury and Baeyens [8]. Our $\log K^0$ value is outside of the range of the $\log K^0$ value based on the LFER (3.0 ≤ $\log K^0$ ≤ 3.8).

The optimized value of $\log K^0$ (−19.5 ± 0.5) for $\equiv SOH + UO_2^{2+} + 3H_2O \rightleftarrows \equiv SOUO_2(OH)_3^{2-} + 4H^+$ was consistent with the values reported by literature [8,11,19], but we could reproduce the experimental data by 2SPNE SC/CE model without considering the surface complexation reactions $\equiv SOH + UO_2^{2+} + H_2O \rightleftarrows \equiv SOUO_2OH + 2H^+$ and $\equiv SOH + UO_2^{2+} + 2H_2O \rightleftarrows \equiv SOUO_2(OH)_2 + 3H^+$. Our results suggested that the sorption of U(VI) on MX-80 bentonite in Na–Ca–Cl solutions at pH_m between 4 and 9, and I between 0.1 and 3 m, could be simulated well by two inner-sphere surface complexation reactions. Stockmann et al. [19] used the PSI/Nagra thermodynamic database version 12/07. We used the latest version of the JAEA thermodynamic database. Both databases included uranium data based on the NEA TDB and are regularly updated. However, it is possible that the two databases may have different thermodynamic parameters for uranium in the Na–Ca–Cl system. The effect of the selection of thermodynamic data/database on the sorption mechanisms of U(VI) on MX-80 will be investigated in future research.
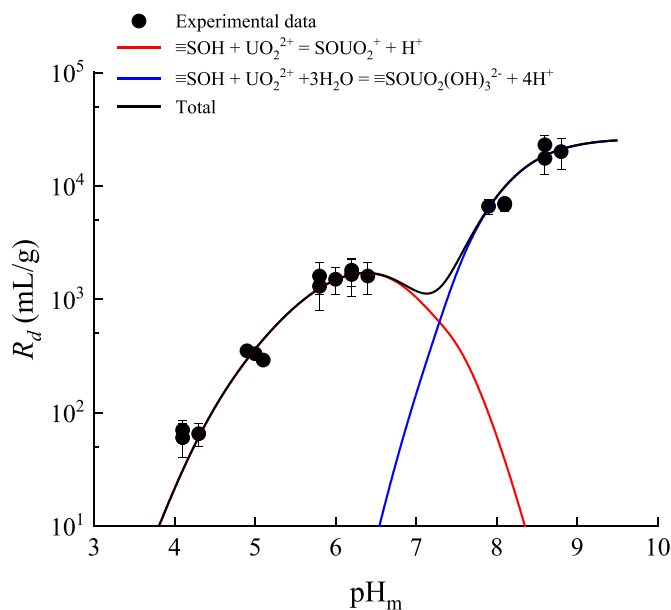

Fig. 3. Fitting results for U(VI) sorption on MX-80 bentonite in ionic strength 3 m Na–Ca–Cl solution with the 2SPNE SC/CE model. The red and blue lines represent $\equiv SOH + UO_2^{2+} \rightleftarrows \equiv SOUO_2^+ + H^+$, and $\equiv SOH + UO_2^{2+} + 3H_2O \rightleftarrows \equiv SOUO_2(OH)_3^{2-} + 4H^+$, respectively. The black line represents the total of modelled sorption. Initial concentration of U(VI) = 1 x 10^{-6} m. Solid/liquid ratio = 0.3 g/30 mL. Temperature = 25 °C. (For interpretation of the references to colour in this figure legend, the reader is referred to the Web version of this article.)

Table 3
Comparison of surface complexation constants $\log K^0$ of U(VI) on montmorillonite obtained in this research with literature values.

Surface complexation reation	$\log K^0$ (this work)[a]	$\log K^0$ [19],[b]	$\log K^0$ [11]	$\log K^0$ [8]
$\equiv SOH + UO_2^{2+} \rightleftarrows \equiv SOUO_2^+ + H^+$	2.3 ± 0.1	2.42 ± 0.04	3.1	3.1
$\equiv SOH + UO_2^{2+} + H_2O \rightleftarrows \equiv SOUO_2OH + 2H^+$	–	-4.49 ± 0.7	-4.6	-3.4
$\equiv SOH + UO_2^{2+} + 2H_2O \rightleftarrows \equiv SOUO_2(OH)_2 + 3H^+$	–	–	-12.6	-11.0
$\equiv SOH + UO_2^{2+} + 3H_2O \rightleftarrows \equiv SOUO_2(OH)_3^{2-} + 4H^+$	-19.5 ± 0.5	-20.5 ± 0.4	-20.9	-20.5

References [8,11] did not provide errors.
[a] Errors correspond to the standard error.
[b] Errors correspond to $\pm 2\sigma$.

3.3. Sorption on illite

Fig. 4 shows the pH_m and I dependences of R_d values of U(VI) sorption onto illite in Na–Ca–Cl solutions (See Fig. S6 in the Supplementary Materials for plots of percentage sorbed). The R_d values increased with increasing pH_m until $pH_m = 7$, where the maximum value of R_d is observed. Then, the R_d values decreased slightly as pH_m increased. The dependence of the R_d value on I could be considered negligible at $I = 0.1$–6 m. Bradbury and Baeyens [20] reported a similar pH dependence of U(VI) sorption onto illite in 0.1 M NaClO$_4$ solution. The pH dependence of U(VI) sorption on illite observed in this study is also similar to those reported by Gao et al. [23] and Montavon et al. [25]. On the other hand, Gao et al. [23] reported a strong I dependence of U(VI) sorption onto the illite provided by ChengMing Illite Co., LTD at $I \leq 0.1$ M (0.001, 0.01 and 0.1 M NaNO$_3$ solution) in the pH range of 2–10, which was attributable to the effect of competing ion exchange. However, as discussed later, the effect of cation exchange was found to be negligible at $pH_m \geq 4$ for the IMt-2 Na-illite we used. Furthermore, this study investigated the effect of I on sorption in more saline Na–Ca–Cl solutions with $I = 0.1$–6 m. These different experimental conditions might explain the different I dependence of U(VI) sorption observed in this work compared to that observed by Gao et al. [23].

The R_d value of U(VI) on illite in the SR-270-PW reference groundwater was measured as $9.8 \times 10^3 \pm 1.1 \times 10^3$ mL/g ($pH_m = 6.1$) and is included in Fig. 4. This is within the range of the R_d values measured in
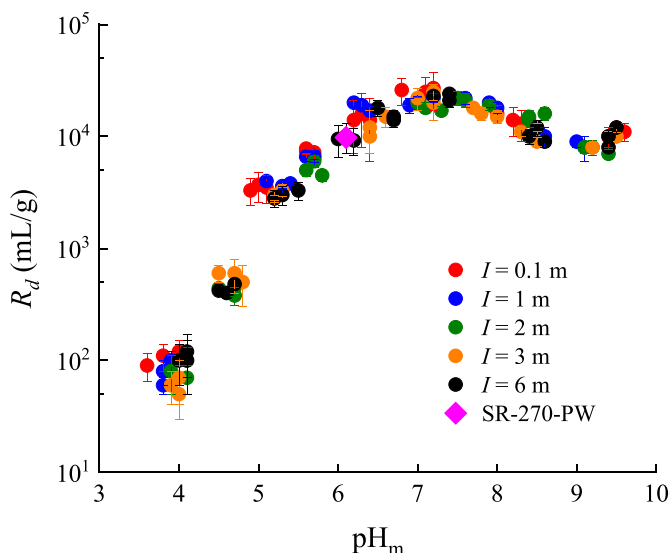
the Na–Ca–Cl solutions at pH_m around 6, suggesting that the impact of minor ions such as Mg^{2+}, K^+, Sr^{2+}, SO_4^{2-} and HCO_3^- on the sorption of U(VI) on illite at pH_m around 6 would be small.

The 2SPNE SC/CE model was applied to the experimental data of the pH_m and I dependences of R_d values of U(VI) sorption onto illite at $I \leq 3$ m shown in Fig. 4. To initiate the fitting of the model, the values of $\log K^0$ and the value of the selectivity coefficient of cation exchange reaction ($\log K_{cation\ exchange} = 0.65$) reported by Bradbury and Baeyens [20] were used as the initial values. Values of other parameters such as protolysis constants and specific surface area were the same as those used by Walker et al. [31] and were held constant during the fitting. Only strong sites of illite were considered for modelling surface complexation reactions at trace concentrations of U(VI).

The fitting results for the sorption of U(VI) on illite in $I = 3$ m Na–Ca–Cl solution with the 2SPNE SC/CE model are illustrated in Fig. 5. Other fitting results at $I = 0.1$, 1 and 2 m are shown in Supplementary Materials (Figs. S7–S9). The optimized values of $\log K^0$ for U(VI) sorption on illite obtained in this study and those by Bradbury and Baeyens [20] are summarized in Table 4.

It was found that the 2SPNE SC/CE model effectively simulated the experimental results of pH_m and I dependences of U(VI) sorption on illite in Na–Ca–Cl solutions. The identified surface complexation reactions and optimized values of $\log K^0$ for the surface complexation reactions agreed well with those reported by Bradbury and Baeyens [20]. It was also found that the contribution of cation exchange reactions to the sorption of U(VI) on illite was negligibly small at $pH_m \geq 4$. This is consistent with the result by Bradbury and Baeyens [20]. The negligible contribution of cation exchange reactions to the sorption of U(VI) on illite explains the insignificant I dependence of U(VI) sorption onto illite as shown in Fig. 4. Consequently, the four inner-sphere surface complexation reactions simulated well the pH_m and I dependences of U(VI) sorption on illite, and the optimized $\log K^0$ values are shown in Table 4.

Fig. 4. pH_m and ionic strength dependences of R_d value of U(VI) sorption on illite in Na–Ca–Cl solutions. Initial concentration of U(VI) = 1×10^{-6} m. Solid/liquid ratio = 0.3 g/30 mL. Temperature = 25 °C.
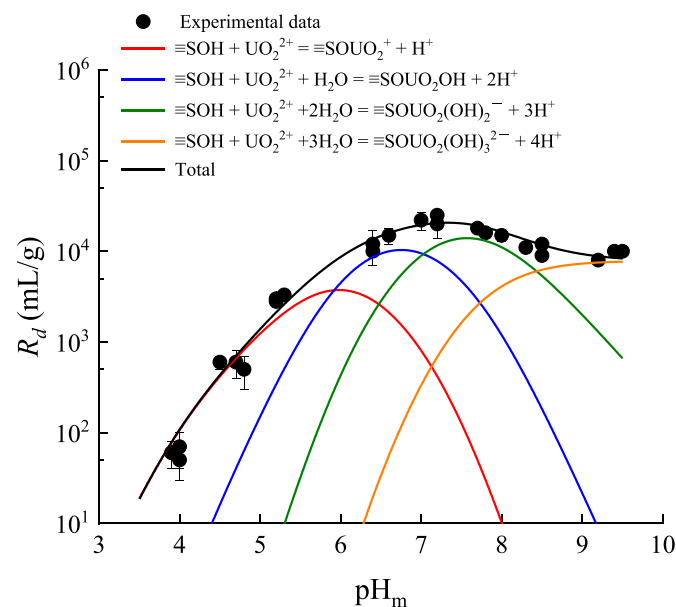

Fig. 5. Fitting results for sorption of U(VI) on illite in ionic strength 3 m Na–Ca–Cl solution with 2SPNE SC/CE model. The red, blue, green, and orange lines represent $\equiv SOH + UO_2^{2+} \rightleftarrows \equiv SOUO_2^+ + H^+$, $\equiv SOH + UO_2^{2+} + H_2O \rightleftarrows \equiv SOUO_2OH + 2H^+$, $\equiv SOH + UO_2^{2+} + 2H_2O \rightleftarrows \equiv S_BOUO_2(OH)_2 + 3H^+$, and $\equiv SOH + UO_2^{2+} + 3H_2O \rightleftarrows \equiv SOUO_2(OH)_3^{2-} + 4H^+$, respectively. The black line represents the total of modelled sorption. Initial concentration of U(VI) = 1×10^{-6} m. Solid/liquid ratio = 0.3 g/30 mL. Temperature = 25 °C. (For interpretation of the references to colour in this figure legend, the reader is referred to the Web version of this article.)

Table 4
Comparison of surface complexation constants log K^0 of U(VI) sorption on illite obtained in this work with literature values.

Surface complexation reaction	log K^0 (this work)[a]	log K^0 [20]
$SOH + UO_2^{2+} \rightleftarrows SOUO_2^+ + H^+$	2.5 ± 0.3	2.0
$SOH + UO_2^{2+} + H_2O \rightleftarrows SOUO_2OH + 2H^+$	-3.4 ± 0.1	-3.5
$SOH + UO_2^{2+} + H_2O \rightleftarrows SOUO_2(OH)^- + 3H^+$	-10.4 ± 0.2	-10.6
$SOH + UO_2^{2+} + 3H2O \rightleftarrows SOUO_2(OH)_3^{2-} + 4H^+$	-18.8 ± 0.2	-19.0

Reference [20] did not provide errors.
[a] Errors correspond to the standard error.

3.4. Sorption on shale and limestone

The results of U(VI) sorption on shale and limestone in I = 0.1–6 m Na–Ca–Cl solutions at pH$_m$ = 4–9 and 5–9 are illustrated in Figs. 6 and 7, respectively (Figures with percentage sorbed are shown in Figs. S10 and S11, respectively). It was found that the effect of I on the sorption of U (VI) on shale at pH$_m$ = 4–9 and on limestone at pH$_m$ = 5–9 was negligible.

The pH$_m$ dependence of U(VI) sorption on shale was similar to that on illite (Fig. 4) probably because illite is the major sorbing clay constituent of the Queenston shale. The extent of the decrease of R_d with pH at pH > 7 was slightly more pronounced for shale than for illite. The reason is not clear at present, but a possible explanation could be that the contributions of two surface complexation reactions ($\equiv SOH + UO_2^{2+} + 2H_2O \rightleftarrows \equiv S_BOUO_2(OH)_2^- + 3H^+$ and $\equiv SOH + UO_2^{2+} + 3H_2O \rightleftarrows \equiv SOUO_2(OH)_3^{2-} + 4H^+$) are smaller for shale than for illite. The Queenston shale used in this study is primarily composed of clay minerals (about 60 % illite, 24 % chlorite, and 10 % illite/smectite) and calcite with minor amounts of quartz and dolomite and trace amounts of gypsum, anhydrite, halite, hematite and goethite [40]. Therefore, an alternative explanation may be that U(VI) formed complexes with carbonate released from calcite and dolomite at pH > 7 during the sorption experiments, leading to the R_d value of U(VI) on shale decreased more pronouncedly than on illite.

The R_d value of U(VI) sorption on limestone increased up to pH$_m$ = 8 and then appeared to be constant at pH$_m$ = 8–9. The limestone used in this work is primarily composed of calcite with minor amounts of dolomite and quartz and trace amounts of anhydrite, pyrite, halite, hematite and goethite [40]. Dolomite can release carbonate into the solution. The R_d value of U(VI) sorption on limestone did not decrease with
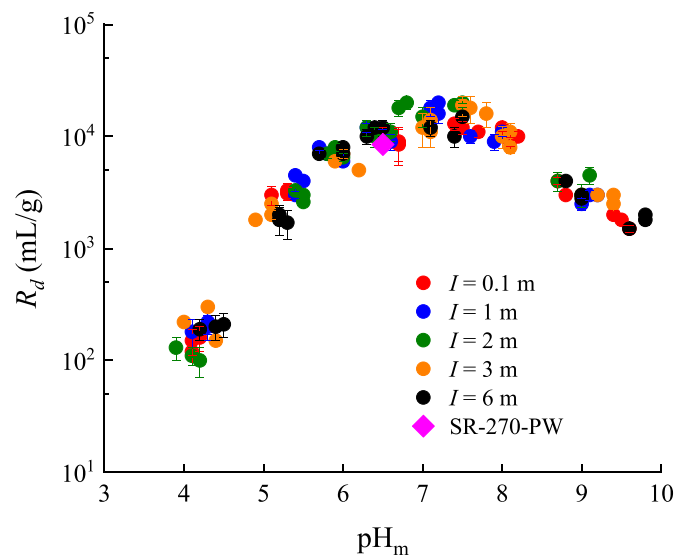

Fig. 6. pH$_m$ and ionic strength dependences of R_d value of U(VI) sorption on shale in Na–Ca–Cl solutions. Initial concentration of U(VI) = 1 x 10^{-6} m. Solid/liquid ratio = 0.3 g/30 mL. Temperature = 25 °C.
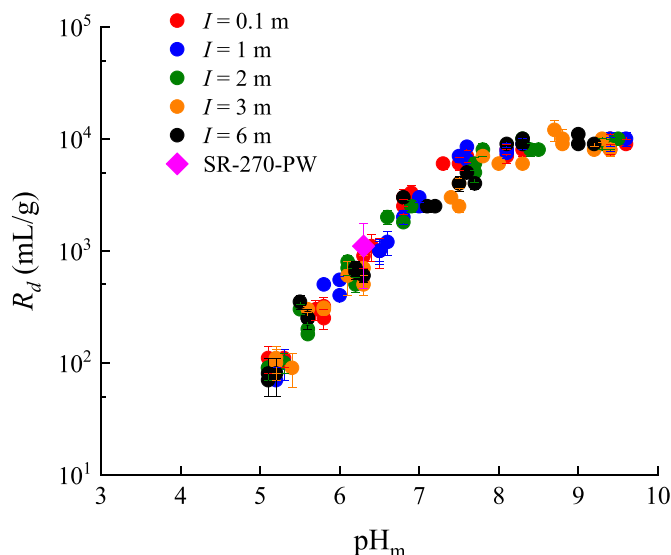

Fig. 7. pH$_m$ and ionic strength dependences of R_d value of U(VI) sorption on limestone in Na–Ca–Cl solutions. Initial concentration of U(VI) = 1 x 10^{-6} m. Solid/liquid ratio = 0.3 g/30 mL. Temperature = 25 °C.

pH$_m$ in the neutral to alkaline pH$_m$ range. Hence the effect of the presence of minor dolomite on the sorption of U(VI) was considered negligible in this study.

Zuo et al. [30] reported that the R_d value of U(VI) sorption on shale in a Ca–HCO$_3$ type water (salinity of 319 mg/L, I of about 0.006 m) was about 720 mL/g at pH = 4, increased slowly with pH, became about 900 mL/g at pH = 8, then increased sharply with pH and reached 1350 mL/g at pH = 10. This trend was not observed in this work. Zhang et al. [27] and Kim et al. [29] studied the sorption of U(VI) on weathered saprolite which was derived from interbedded shale, limestone and sandstone sequences in 0.05 M NaNO$_3$ solution at equilibrium with atmospheric CO$_2$ at solid/liquid ratio = 0.005 and 0.25 kg/L. The pH$_m$ dependence of U(VI) sorption onto shale measured at solid/liquid ratio = 0.3 g/30 mL in this study was qualitatively similar to the pH dependence of U(VI) sorption on weathered shale saprolite measured at solid/liquid ratio = 0.005 kg/L but was completely different from that measured at solid/-liquid ratio = 0.25 kg/L by Zhang et al. [27] and Kim et al. [29]. The pH$_m$ dependence of U(VI) sorption onto limestone did not agree with the results of U(VI) sorption on weathered limestone saprolite by Zhang et al. [27] or Kim et al. [29]. This might be due to the difference in the degree of carbonate complex formation in the solid/liquid ratio = 0.005 and 0.25 kg/L experiments and due to the different mineralogical components in the shale and limestone used in this work compared to those in the weathered saprolite used by Zhang et al. [27] and Kim et al. [29]. The saprolite is primarily composed of quartz, illite, and potassium feldspar with minor amounts of hydroxy interlayered vermiculite, vermiculite, goethite, lepidocrocite, ferrihydrite, and kaolinite [29]. The Na–Ca–Cl solution used in this work is also different from the NaNO$_3$ solution used by Zhang et al. [27] and Kim et al. [29].

There is no data for the protonation and de-protonation of mineral components of the Queenston shale and limestone we used. In the future, we will attempt to elucidate the surface properties of the mineral components including minor minerals of Queenston shale and limestone and study the sorption mechanisms of U(VI) on shale and limestone by applying the 2SPNE SC/CE model.

The R_d values of U(VI) on Queenston shale and limestone in the SR-270-PW reference groundwater were measured as 8.5 x 10^3±1.0 x 10^3 mL/g (pH$_m$ = 6.5) and 1.1 x 10^3±6.4 x 10^2 mL/g (pH$_m$ = 6.3), respectively. These are included in Figs. 6 and 7, respectively. These are within the range of the R_d values measured in the Na–Ca–Cl solutions at pH$_m$ of around 6, suggesting that the impact of minor ions such as Mg^{2+}, K$^+$,

Sr^{2+}, SO_4^{2-} and HCO_3^- on the sorption of U(VI) on shale and limestone at pH_m about 6 would be small.

4. Conclusions

In the present study, the sorption behavior of U(VI) on MX-80 bentonite, illite, shale and limestone in Na–Ca–Cl solutions with I of 0.1–6 m in a CO_2 free environment at pH_m of 4–9 for MX-80 bentonite, illite and shale and at pHm = 5–9 for limestone was systematically elucidated. Furthermore, the pH_m and I dependences of the R_d value of U(VI) sorption on MX-80 and illite in Na–Ca–Cl solutions were successfully simulated with the 2SPNE SC/CE model.

Sorption kinetics were observed for all four solids at $I = 0.1$ m and 6 m. It was found that the sorption of U(VI) reached equilibrium within 7 days on all four solids. It was also confirmed that U(VI) sorption on all four solids was independent of the I in the range of 0.1–6 m. U(VI) sorption on MX-80 bentonite showed that the R_d values increased with increasing pH_m until $pH_m = 6$. Then, the R_d value decreased slightly as pH_m increased until $pH_m = 7$, but R_d increased again with increasing pH_m until $pH_m = 9$. The R_d value of U(VI) sorption on illite increased with increasing pH_m until $pH_m = 7$, where the maximum value of R_d was observed. The R_d value then decreased slightly as pH_m increased. The sorption behavior of U(VI) on shale was similar to that on illite, but the extent of decrease in R_d value at $pH_m > 7$ was slightly larger for shale than for illite. The R_d value of U(VI) sorption on limestone increased with pH_m up to $pH_m = 8$ and then appeared to be constant at $pH_m = 8$–9. The similar R_d values determined for U(VI) sorption in Na–Ca–Cl solutions and in the SR-270-PW reference groundwater illustrates that the impact of minor ions in solution such as Mg^{2+}, K^+, Sr^{2+}, SO_4^{2-} and HCO_3^- on the sorption of U(VI) onto all four solids at pH_m around 6 was small. By applying the 2SPNE SC/CE model to the sorption of U(VI) onto MX-80 bentonite and illite, two inner-sphere surface complexation reactions and four inner-sphere surface complexation reactions were identified for U(VI) sorption onto MX-80 bentonite and illite, respectively. The optimized value of log K^0 of each surface complexation reaction was evaluated.

Declaration of generative AI in scientific writing

Authors did not use of any AI tools to analyze and draw insights from data as part of the research process.

CRediT authorship contribution statement

Zhiwei Zheng: Formal analysis, Data curation. **Jianan Liu:** Formal analysis, Data curation. **Shinya Nagasaki:** Writing – original draft, Supervision, Project administration, Methodology, Investigation, Funding acquisition, Conceptualization. **Tammy Yang:** Writing – review & editing, Validation, Supervision.

Declaration of competing interest

No potential conflict of interest was reported by the authors.

Acknowledgments

Appendix A. Supplementary data

Supplementary data to this article can be found online at https://doi.org/10.1016/j.net.2024.06.036.

References

[1] H. Geckeis, J. Lützenkirchen, R. Polly, T. Rabung, M. Schmidt, Mineral-water interface reactions of actinides, Chem. Rev. 113 (2013) 1016–1062, https://doi.org/10.1021/cr300370h.

[2] J.K. Lee, M.H. Baik, J.W. Choi, M.S. Seo, Development of a web-based sorption database (KAERI-SDB) and application to the safety assessment of a radioactive waste disposal, Nucl. Eng. Des. 241 (2011) 5316–5324, https://doi.org/10.1016/j.nucengdes.2011.09.045.

[3] National Academy of Science, A study of the isolation for geologic disposal of radioactive wastes, Waste Isolation Systems Panels, in: Board on Radioactive Waste Management, 1983. Washington DC, USA.

[4] J. Noronha, Deep Geological Repository Conceptual Design Report, Crystalline/Sedimentary Rock Environment, Technical Report, Nuclear Waste Management Organization, May 2016. APM-REP-00440-0015 R001.

[5] M.Y. Hobbs, S.K. Frape, O. Shouakar-Stash, L.R. Kennell, Regional Hydrogeochemistry - Southern Ontario, Technical Report, Nuclear Waste Management Organization, Toronto, Canada, 2011. NWMO DGR-TR-2011-12.

[6] P. Vilks, T. Yang, Sorption of selected radionuclides on sedimentary rocks in saline conditions – updated sorption values, in: Technical Report, Nuclear Waste Management Organization, 2018. NWMO-TR-2018-03, Toronto, Canada.

[7] R. Pabalan, D.R. Turner, Uranium(6+) sorption on montmorillonite: experimental and surface complexation modeling study, Aquat. Geochem. 2 (1997) 203–226.

[8] M.H. Bradbury, B. Baeyens, Modelling the sorption of Mn(II), Co(II), Ni(II), Zn(II), Cd(II), Eu(III), Am(III), Sn(IV), Th(IV), Np(V) and U(VI) on montmorillonite: linear free energy relationships and estimates of surface binding constants for some selected heavy metals and actinides, Geochem. Cosmochim. Acta 69 (2005) 875–892, https://doi.org/10.1016/j.gca.2004.07.020.

[9] M. Majdan, S. Pikus, A. Gajowiak, A. Gładysz-Płaska, H. Krzyżanowska, J. Żuk, M. Bujacka, Characterization of uranium(VI) sorption by organobentonite, Appl. Surf. Sci. 256 (2010) 5416–5421, https://doi.org/10.1016/j.apsusc.2009.12.123.

[10] X. Ren, S. Wang, S. Yang, J. Li, Influence of contact time, pH, soil humic/fulvic acids, ionic strength and temperature on sorption of U(VI) onto MX-80 bentonite, J. Radioanal. Nucl. Chem. 283 (2010) 253–259, https://doi.org/10.1007/s10967-009-0323-0.

[11] M. Marques Fernandes, B. Baeyens, R. Dähn, A.C. Scheinost, M.H. Bradbury, U(VI) sorption on montmorillonite in the absence and presence of carbonate: a macroscopic and microscopic study, Geochimiica et Cosmochimica Acta 93 (2012) 262–277, https://doi.org/10.1016/j.gca.2012.04.017.

[12] J. Xiao, Y. Chen, W. Zhao, J. Xu, Sorption behavior of U(VI) onto Chinese bentonite: effect of pH, ionic strength, temperature and humic acid, J. Mol. Liq. 188 (2013) 178–185, https://doi.org/10.1016/j.molliq.2013.10.008.

[13] P.K. Verma, P. Pathak, M. Mohapatra, A.K. Yadav, S. Jha, D. Bhattacharyya, P.K. Mohapatra, Spectroscopic investigations on sorption of uranium onto suspended bentonite: effects of pH, ionic strength and complexing anions, Radiochim. Acta 103 (2015) 293–303, https://doi.org/10.1515/ract-2014-2309.

[14] S. Li, X. Wang, Z. Huang, L. Du, Z. Tan, Y. Fu, X. Wang, Sorption and desorption of uranium(VI) on GMZ bentonite: effect of pH, ionic strength, foreign ions and humic substances, J. Radioanal. Nucl. Chem. 308 (2016) 877–886, https://doi.org/10.1007/s10967-015-4513-7.

[15] J. Zheng, D. Luo, Y. Qiao, L. Wang, W. Wu, C. Zhang, Y. Ye, Surface complexation modeling of U(VI) sorption on GMZ bentonite in the presence of fulvic acid, Radiochim. Acta 105 (2017) 33–41, https://doi.org/10.1515/ract-2016-2654.

[16] Q. Zuo, X. Gao, J. Yang, P. Zhang, G. Chen, Y. Li, K. Shi, W. Wu, Investigation on the thermal activation of montmorillonite and its application for the removal of U(VI) in aqueous solution, Journal of Taiwan Institute of Chemical Engineering 80 (2017) 754–760, https://doi.org/10.1016/j.jtice.2017.09.016.

[17] T. Philipp, S.S.A. Azzam, A. Rossberg, N. Huittinen, K. Schmeide, T. Stumpf, U(VI) sorption on Ca-bentonite at (hyper)alkaline conditions – spectroscopic investigations of retention mechanisms, Sci. Total Environ. 676 (2019) 469–481, https://doi.org/10.1016/j.scitotenv.2019.04.274.

[18] K. Brix, S. Baur, A. Haben, R. Kautenburger, Building the bridge between U(VI) and Ca-bentonite – Influence of concentration, ionic strength, pH, clay composition and competing ions, Chemosphere 285 (2021) 131445, https://doi.org/10.1016/j.chemosphere.2021.131445.

[19] M. Stockmann, K. Fritsch, F. Bok, M. Marques Fernandes, B. Baeyens, R. Steudtner, K. Müller, C. Nebelung, V. Brendler, T. Stumpf, K. Schmeide, New insights into U(VI) sorption onto montmorillonite from batch sorption and spectroscopic studies at increased ionic strength, Sci. Total Environ. 806 (2022) 150653, https://doi.org/10.1016/j.scitotenv.2021.150653.

[20] M.H. Bradbury, B. Baeyens, Sorption modelling on illite. Part II: Actinide sorption and linear free energy relationships, Geochem. Cosmochim. Acta 73 (2009) 1004–1013, https://doi.org/10.1016/j.gca.2008.11.016.

[21] M. Marques Fernandes, N. Vér, B. Baeyens, Predicting the uptake of Cs, Co, Ni, Eu, Th and U on argillaceous rocks using sorption models for illite, Appl. Geochem. 59 (2015) 189–199, https://doi.org/10.1016/j.apgeochem.2015.05.006.

[22] M.H. Bradbury, B. Baeyens, Experimental and Modelling Investigations on Na-Illite: Acid–Base Behaviour and the Sorption of Strontium, Nickel, Europium and Uranyl, PSI Bericht Nr. 05-02. Paul Scherrer Institut, Villigen and NTB 04-02, Nagra, Wettingen, Switzerland, 2005.

[23] Y. Gao, Z. Shao, Z. Xiao, U(VI) sorption on illite: effect of pH, ionic strength, humic acid and temperature, J. Radioanal. Nucl. Chem. 303 (2015) 867–876, https://doi.org/10.1007/s10967-014-3385-6.

[24] R. Liao, Z. Shi, Y. Chen, J. Zhang, X. Wang, Y. Hou, K. Zhang, Characteristics of uranium sorption on illite in a ternary system: effect of phosphate on adsorption,

J. Radioanal. Nucl. Chem. 323 (2020) 159–168, https://doi.org/10.1007/s10967-019-06878-y.

[25] G. Montavon, S. Ribet, Y. Hassan Loni, F. Maia, C. Bailly, K. David, C. Lerouge, B. Madé, J.C. Robinet, B. Grambow, Uranium retention in a Callovo-Oxfordian clay rock formation: from laboratory-based models to in natura conditions, Chemosphere 299 (2022) 134307, https://doi.org/10.1016/j.chemosphere.2022.134307.

[26] H. Mei, N. Aoyagi, T. Saito, N. Kozai, Y. Sugiura, Y. Tachi, Uranium (VI) sorption on illite under varying carbonate concentrations: batch experiments, modeling, and cryogenic time-resolved laser fluorescence spectroscopy study, Applied Geochemisty 136 (2022) 105178, https://doi.org/10.1016/j.apgeochem.2021.105178.

[27] F. Zhang, J.C. Parker, S.C. Brooks, Y.-J. Kim, G. Tang, P.M. Jardine, D.B. Watson, Comparison of approaches to calibrate a surface complexation model for U(VI) Sorption to Weathered Saprolite, Transport Porous Media 78 (2009) 185–197, https://doi.org/10.1007/s11242-008-9294-9.

[28] S. Ortaboy, G. Atun, Kinetics and equilibrium modeling of uranium(VI) sorption by bituminous shale from aqueous solution, Ann. Nucl. Energy 73 (2014) 345–354, https://doi.org/10.1016/j.anucene.2014.07.003.

[29] Y.-J. Kim, S.C. Brooks, F. Zhang, J.C. Parker, J.-W. Moon, Y. Roh, Fate and transport of uranium(VI) in weathered saprolite, J. Environ. Radioact. 139 (2015) 154–162, https://doi.org/10.1016/j.jenvrad.2014.10.008, 2015.

[30] R. Zuo, L. Wang, R. Shi, J. Yang, J. Wang, Y. Teng, Factors influencing the sorption and migration behavior of uranium in shale, J. Radioanal. Nucl. Chem. 314 (2017) 887–896, https://doi.org/10.1007/s10967-017-5448-y.

[31] A. Walker, J. Racette, T. Saito, T. Yang, S. Nagasaki, Sorption of Se(-II) on illite, MX-80 bentonite, shale, and limestone in Na-Ca-Cl solution, Nucl. Eng. Technol. 54 (2022) 1616–1622, https://doi.org/10.1016/j.net.2021.10.039.

[32] M. Altmaier, V. Metz, V. Neck, R. Müller, T. Fanghänel, Solid-liquid equilibria of $Mg(OH)_2(cr)$ and $Mg_2(OH)_3Cl \cdot 4H_2O(cr)$ in the system mg-na-H-OH-Cl-H_2O at 25°C, Geochem. Cosmochim. Acta 67 (2003) 3595–3601, https://doi.org/10.1016/S0016-7037(03)00165-0.

[33] M. Altmaier, V. Neck, T. Fanghänel, Solubility of Zr(IV), Th(IV) and Pu(IV) hydrous oxides in $CaCl_2$ solutions and the formation of ternary Ca-M(IV)-OH complexes, Radiochim. Acta 96 (2008) 541–550, https://doi.org/10.1524/ract.2008.1535.

[34] S. Nagasaki, J. Riddoch, T. Saito, J. Goguen, A. Walker, T.T. Yang, Sorption behaviour of Np(IV) on illite, shale and MX-80 in high ionic strength solutions, J. Radioanal. Nucl. Chem. 313 (2017) 1–11, https://doi.org/10.1007/s10967-015-4332-x.

[35] D.L. Parkhurst, C.A.J. Appelo, Description of Input and Examples for PHREEQC Version 3 - a Computer Program for Speciation, Batch-Reaction, One-Dimensional Transport, and Inverse Geochemical Calculations, U.S. Geological Survey Techniques and Methods, 2013. Book 6, Chap. A43.

[36] Japan Atomic Energy Agency, Thermodynamic DataBase. https://migrationdb.jaea.go.jp/english.html, April 27, 2021. (Accessed 9 December 2023).

[37] Y. Sugiura, T. Ishidera, Y. Tachi, Surface complexation of Ca and competitive sorption of divalent cations on montmorillonite under alkaline conditions, Appl. Clay Sci. 200 (2021) 105910, https://doi.org/10.1016/j.clay.2020.105910.

[38] M.H. Bradbury, B. Baeyens, A mechanistic description of Ni and Zn sorption on Na-montmorillonite Part II: modelling, Journal of Conatminant Hydrology 27 (1997) 223–248. https://doi-org.libaccess.lib.mcmaster.ca/10.1016/S0169-7722(97)00007-7.

[39] L. Ciavatta, The specific interaction theory in the evaluating ionic equilibria, Annali di Chimica (Rome) 70 (1980) 551–567.

[40] Intera Engineering Ltd, OPG's Deep Geologic Repository for Low & Intermediate Level Waste, Technical Report, Nuclear Waste Management Organization, Toronto, Canada, 2011. NWMO DGR-TR-2011-24.